

# Status of LHCb and Prospects for Charm Physics

S. Barsuk<sup>\*†1</sup>

<sup>1</sup>on behalf of the LHCb collaboration

**Abstract: The LHCb experiment at the LHC is fully installed, its commissioning is being completed. Commissioning of the detector with cosmic rays and the first experience with the LHC particles is reported. Prospects of the LHCb experiment to study rare phenomena in charm physics sector are discussed.**

## Introduction

LHCb is an experiment dedicated to studies of rare phenomena in  $b$  and  $c$  decays in order to precisely constrain the Standard Model parameters and search for signatures beyond [1]. The  $b$  and  $c$  hadrons are produced from the collisions of the LHC  $p$  beams with nominal center of mass energy  $E_{CM} = 14$  TeV. The LHCb operation is foreseen at a reduced LHC luminosity of  $2 \times 10^{32} \text{ cm}^{-2} \text{ s}^{-1}$ , tuneable by defocusing beams in order to maximize a single interaction probability per beam crossing. Using a  $10^7$  s effective annual operation time and assumed  $\sigma_{b\bar{b}} = 1.04$  mb and  $\sigma_{c\bar{c}} = 8.31$  mb cross sections, this translates into the integrated luminosity of  $2 \text{ fb}^{-1}$  and samples of  $10^{12}$   $b\bar{b}$  pairs and  $6 \times 10^{12}$   $c\bar{c}$  pairs annually produced. Throughout the paper this is referred to as a nominal year of LHCb operation.

During 2010, the first year of LHC operation, the machine is expected to operate at the reduced energy starting from  $E_{CM} = 7$  TeV, which then will be substantially increased. The luminosity in 2010 is foreseen to be significantly lower than that hoped for in previous years, and a data sample of around  $100\text{-}200 \text{ pb}^{-1}$  is expected. The projections for the first LHCb year, done below, imply the energy  $E_{CM} = 10$  TeV corresponding to  $\sigma_{b\bar{b}} = 0.67$  mb and  $\sigma_{c\bar{c}} = 6.26$  mb cross sections, and an integrated luminosity of  $100 \text{ pb}^{-1}$ . Taking into account the variation in production cross section with energy, which is greater for  $b\bar{b}$  events, this corresponds to samples of  $7 \times 10^{10}$   $b\bar{b}$  pairs and  $6 \times 10^{11}$   $c\bar{c}$  pairs.

Charm physics studies at LHCb can exploit two different production mechanisms. The cleanest approach is to reconstruct charm from  $b$ -quark decays with well displaced (on average 7 mm)  $b$ -decay vertex. The event sample, containing secondary charm hadrons, is, however, suppressed by the  $b$  vertex reconstruction efficiency and  $b$ -decay vertex from the  $pp$  interaction vertex separation cut efficiency. The sample purity for  $D^0$  mesons [2] can conveniently be enhanced by selecting the chain of  $B \rightarrow D^{*+}(\rightarrow D^0\pi^+)X$  with a powerful cut on  $\Delta M = M(D^0\pi^+) - M(D^0)$ . In this case, however, the additional suppression

by  $BR(B \rightarrow D^{*+}X)/(BR(B \rightarrow D^{*+}X) + BR(B \rightarrow D^{*0}X)) \times BR(D^{*+} \rightarrow D^0\pi^+) \approx 0.18$  is introduced. An alternative approach is to select prompt charm hadrons. In this case other properties of the reconstructed decay must be used to cope with the combinatorial background. For example,  $D^0$  and  $D_{(S)}^+$  mesons travel about 3 mm and about 10 mm respectively, so that the  $D$  decay vertex can be reconstructed. The prompt  $D^{*+}$  decays to  $D^0\pi^+$  can also be used. In 2010 the integrated luminosity means that all charm studies will exploit the prompt production only.

LHCb is well suited to charm physics. It benefits from its good track and precise vertex reconstruction, its powerful particle identification, its large rapidity coverage, and anticipated very high statistical yields. However, the analysis has to cope with high event multiplicities, forward detector geometry which prevents full event reconstruction, and a trigger compromise between  $b$  and  $c$  physics targets.

## The LHCb Detector

The LHCb detector (Fig. 1) is a single-arm forward spectrometer, covering  $10\text{-}300$  ( $15\text{-}250$ ) mrad acceptance for  $x(y)$  projections. It provides efficient charged particle tracking and neutral particle reconstruction, precise vertex measurement, particle identification and robust trigger. Passing from the  $pp$  interaction region, particles meet a vertex locator (VELO), a 4 Tm warm dipole magnet, a tracking system, two ring imaging Cherenkov detectors (RICH), a system of calorimeters and a muon detector.

The VELO system comprises 21 stations of two semicircular silicon sensors each yielding polar coordinates measurement. The sensors are retractable in order to provide safe conditions during injection and until the stable beams are achieved. At the closed position, the sensitive area of the VELO detectors is as close as 8 mm to the beam axis. In addition to VELO, the LHCb tracking system comprises four planar tracking stations, trigger tracker (TT) upstream of the dipole magnet and T1-T3 stations downstream of the magnet. While TT and the region close to the beam pipe of T1-T3 employ silicon microstrips, the straw tubes are used for the outer region of T1-T3.

A track reconstruction efficiency of 95 % is expected for track momenta  $p > 5$  GeV. Momentum measurement resolution is expected to be  $\Delta p/p \sim 0.4\%$  and is dominated by multiple scattering up to 80 GeV/c (Fig. 2). Primary vertex position resolution is typically 8  $\mu\text{m}$  in the transverse,  $x$  or  $y$ , direction, and 44  $\mu\text{m}$  along the beam axis. The impact parameter measurement has a resolution of  $\sigma_{IP} \sim 30 \mu\text{m}$ , and is dominated by the effect of material before the first measured point (Fig. 3).

A system of two Cherenkov detectors is used for  $K/\pi$

\* barsuk@lal.in2p3.fr

<sup>†</sup> Laboratoire de l'Accélérateur Linéaire, Université Paris-Sud 11, Bât. 200, 91898 Orsay, France

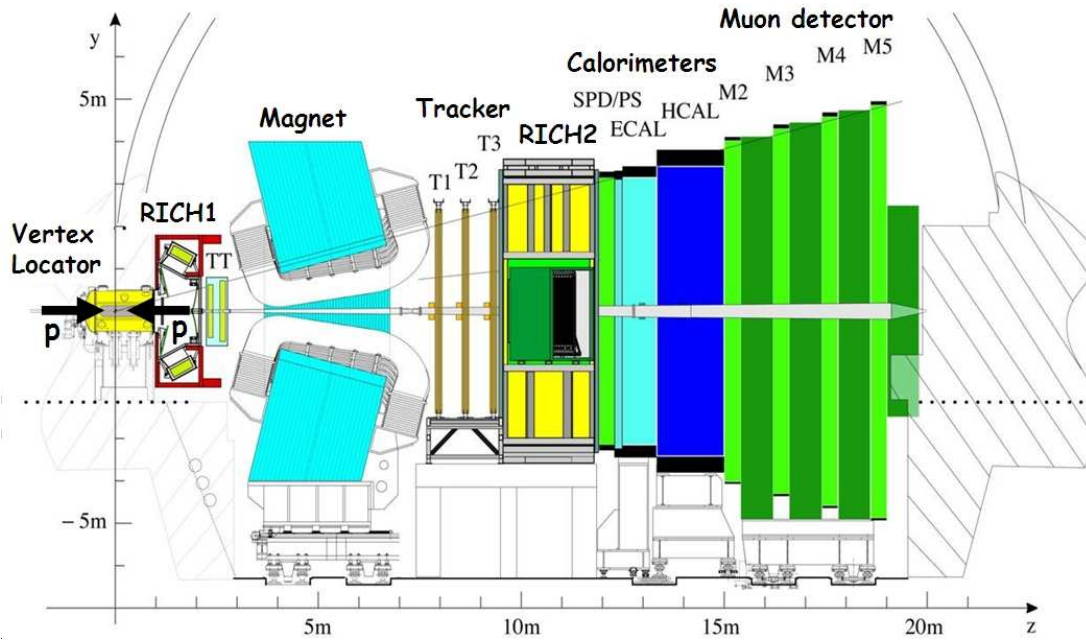


Figure 1: Side view of the LHCb detector from inside of the LHC machine loop

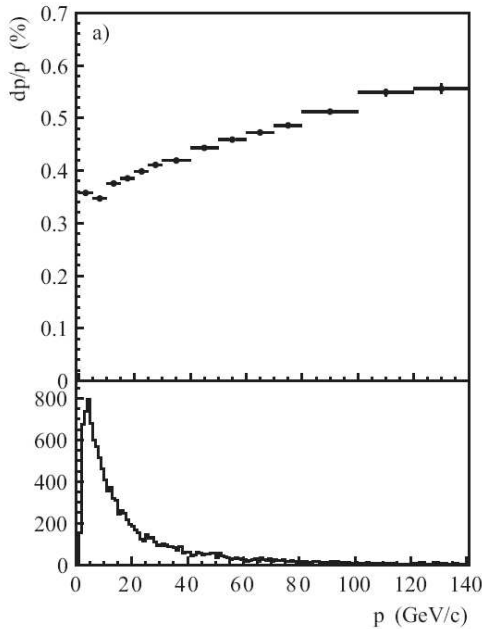


Figure 2: Momentum resolution as a function of track momentum. For comparison the momentum spectrum of  $B$  decay particles is shown in the lower part of the plot

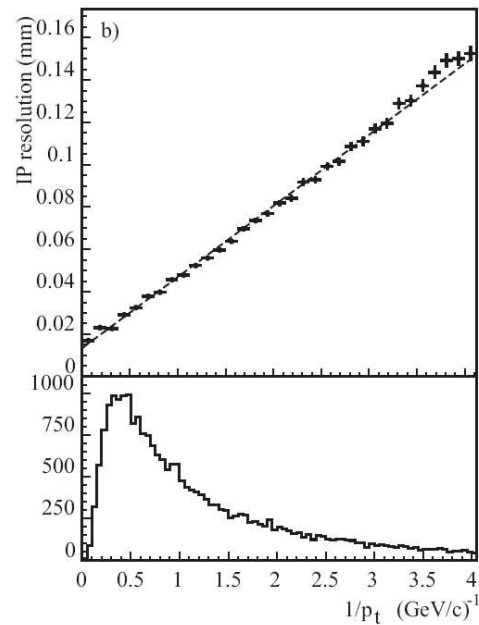


Figure 3: Impact parameter resolution as a function of  $1/p_T$ . For comparison the  $1/p_T$  spectrum of  $B$  decay particles is shown in the lower part of the plot

separation. The RICH1 detector is aimed at the identification of lower momenta particles and so it is installed upstream of the magnet. It covers a momentum range from 1 to about 70 GeV/c in the 25 to 250 (300) mrad vertical (horizontal) acceptance, and uses silica aerogel and  $C_4F_{10}$  as radiators. RICH2 provides identification for particles of 15 to about 100 GeV/c momenta in the 15 to 100 (120) mrad

vertical (horizontal) acceptance, and is positioned downstream of the magnet. It employs a  $CF_4$  radiator.

Excellent  $K/\pi$  separation is expected in the momentum range between 2 and 100 GeV/c with the average  $\pi \rightarrow K$  misidentification rate of 4 % for the  $K$  identification efficiency of 96 % (Fig. 4).

The identification of electrons, photons and hadrons as

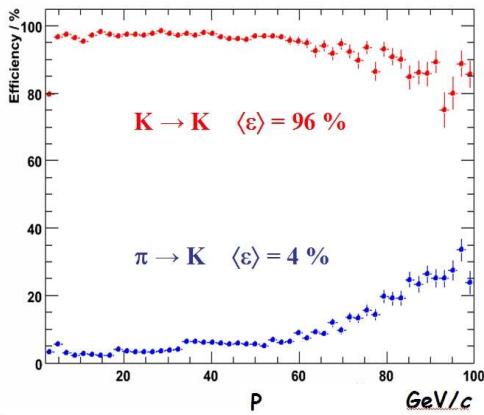


Figure 4: Kaon-pion separation as a function of particle momentum. Top curve shows kaon identification efficiency, and bottom curve describes pion rejection

well as measurement of their energy and position is provided by the calorimeter system. The LHCb calorimeter, however, is essentially a trigger tool, which, along with the muon detector, initiates the trigger search. The calorimeter system comprises scintillator pad detector, pre-shower, electromagnetic and hadronic calorimeters, all employing the sampling technology with the light, produced in the plastic scintillator, and read out to the photomultipliers via wavelength-shifting fibers.

The muon detector performs the offline identification of muons and initiates trigger search for the muon based trigger alleys, and is implemented in five stations, interleaved with the concrete absorber. The MWPC technology is used throughout the muon detector, except for the busy innermost region of the muon station in front of the calorimeter, where the GEM technology has been chosen.

The lowest (L0) trigger level of LHCb is implemented in hardware and uses the information from the calorimeter, the muon detector and VELO. A high  $p_T$  candidate is searched for in the  $h^\pm$ ,  $\mu^\pm$ ,  $\mu^+\mu^-$ ,  $e^\pm$ ,  $\gamma$  and  $\pi^0$  alleys to initiate the further trigger search. A  $p_T$  cut varies from about 1 GeV for muons to about 4.5 GeV for  $\pi^0$ . In addition, it is possible to veto very complicated events, compatible with more than one  $pp$  interaction, using the information from upstream hodoscope counters or scintillator pad detector. The L0 is fully synchronous, runs at 40 MHz, and reduces the 10 MHz input event rate to the rate of 1 MHz output to the high level trigger (HLT). The HLT is fully implemented on a farm of processors, and uses full event information. First, it confirms the L0 candidate with the tracker and VELO measurement (HLT1). Then, inclusive selections run on the globally reconstructed event (HLT2). The HLT reduces event rate to a 2 kHz output for storage. A set of inclusive trigger selections, looking for displaced vertices,  $J/\psi$  candidates and muons with significant impact parameter with respect to primary vertices, will result in a high yield in events containing  $D$  mesons. For a detailed description of the LHCb trigger see e.g. [3].

A more detailed discussion of the LHCb detector can be found elsewhere [4].

## The Detector Commissioning

The detector is fully installed and the commissioning program is being completed. The detector commissioning has exploited cosmic ray muons, particles produced from stopped beams during injection tests, and beam-gas events from the brief period with the first circulating beam in 2008.

Although the LHCb geometry is not ideal for exploiting cosmic ray muons, nonetheless many useful studies can still be performed with such a source. More than one million calorimeter triggered tracks has been collected. The calorimeter detectors gain was increased in order to ensure a measurable MIP signal with these tracks. This sample of reconstructed MIP tracks has been used for the commissioning of the large surface tracking detectors, which include the outer tracker and the muon detector, and the calorimeter. Using this sample of cosmics is difficult or impossible for the inner tracker because of its small size, for the trigger tracker because of the large extrapolation distance, and for the VELO because of both of the above reasons. Readout of consecutive samplings gives a powerful tool for time alignment. The feasibility of the time alignment to about 1 ns precision has been shown.

The LHCb recorded events from the two LHC sector tests with the beam, dumped on the injection line beam stopper about 340 m downstream of the LHCb detector. These induced high muon flux events contained  $O(10)$  particles/cm<sup>2</sup> in the shower center, and  $O(0.1)$  particles/cm<sup>2</sup> in the region of VELO. About 700 tracks, reconstructed in VELO per sector test, served for the spatial alignment of all the LHCb tracking detectors. Fig. 5 shows

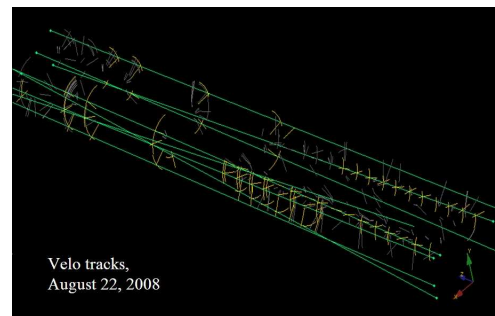


Figure 5: Sector test event. Tracks reconstructed in VELO from the  $r$  and  $\phi$  hits in the VELO sensors

VELO tracks (in green), reconstructed from the hits in the  $r$  and  $\phi$  sensors (in orange). With these data VELO module alignment precision was found to be  $3.4 \mu\text{m}$  for  $x$ ,  $y$  translation and  $200 \mu\text{rad}$  for  $z$  rotation. Residual measurements for  $r$  and  $\phi$  sensors confirm the previous measurements (Fig. 6, 7). Extrapolated VELO tracks were found in the TT within a  $300 \mu\text{m}$  of the expected position. Extrapolation to the inner tracker by a distance of 7 m results,

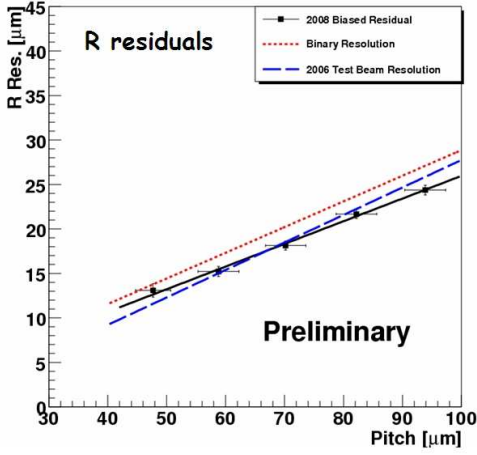


Figure 6:  $r$  residuals measured from the sector test reconstructed tracks, as compared to the previous measurements

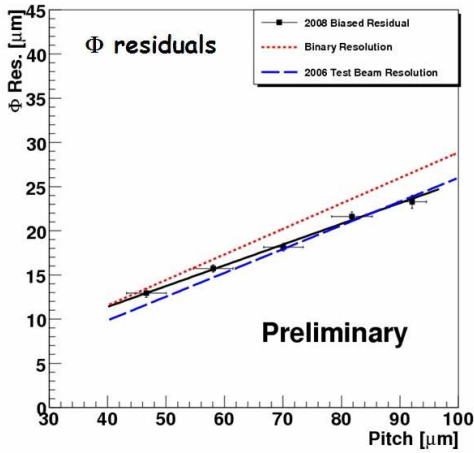


Figure 7:  $\phi$  residuals measured from the sector test reconstructed tracks, as compared to the previous measurements

however, in a large combinatorial background due to high multiplicity of the beam dump events.

The first LHC beam yielded a few low multiplicity beam gas events with about 50 reconstructed tracks per event (Fig. 8), and a few busy events with beam, hitting a collimator (Fig. 9).

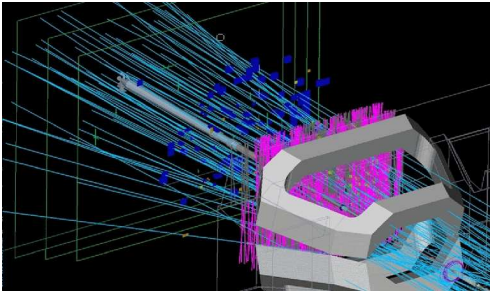


Figure 9: The beam-collimator event collected from the first LHC beam circulation

After this extensive commissioning phase, the LHCb detector is ready for data taking after the LHC restart in autumn 2009.

## Charm Physics Goals

In the remainder of the article, the LHCb reach in the charm sector is illustrated by the simulation studies of mixing and  $CP$  violation using  $D^0 \rightarrow h^+h^-$ ,  $h^+h^-h^+h^-$ , rare  $D$  meson decays,  $B_c^+$  studies, charmonium production and charmonium-like states.

The expected number of  $D^0 \rightarrow h^+h^-$  from  $B$  decays in one nominal LHCb year is shown in Table 1.

Table 1: The expected number of  $D^0 \rightarrow h^+h^-$  from  $B$  decays in one nominal LHCb year

channel	# of events
$D^0 \rightarrow K^- \pi^+$	12.4 M
$D^0 \rightarrow K^- K^+$	1.6 M
$D^0 \rightarrow \pi^- \pi^+$	0.6 M
$D^0 \rightarrow K^+ \pi^-$	0.05 M

As mentioned above, the luminosity in 2010 is foreseen to be significantly lower compared to the nominal one, and a data sample of around  $100\text{-}200 \text{ pb}^{-1}$  is expected. This low luminosity brings, however, some benefits. For example, it will prove possible to lower the  $p_T$  and  $IP$  thresholds in the trigger and significantly boost the efficiency for charm, in particular for prompt events. The expected prolific production of prompt  $D^0$  mesons is illustrated by the Fig. 10, where the invariant mass of

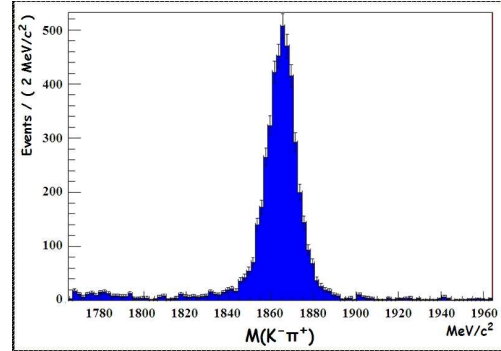


Figure 10: Reconstructed invariant mass of the  $K^- \pi^+$  combinations in the minimum bias sample at  $E_{CM} = 10 \text{ TeV}$  passing the L0 and HLT1 trigger. A cut has been imposed on the reconstructed  $\Delta M = M(D^0 \pi^+) - M(D^0)$ . The sample corresponds to about 15 minutes of data taking in the conditions expected for 2010

the  $K^- \pi^+$  combinations is shown for the minimum bias sample at  $E_{CM} = 10 \text{ TeV}$  passing the L0 and HLT1 trigger, with a cut imposed on the reconstructed  $\Delta M = M(D^0 \pi^+) - M(D^0)$ . The sample corresponds to about



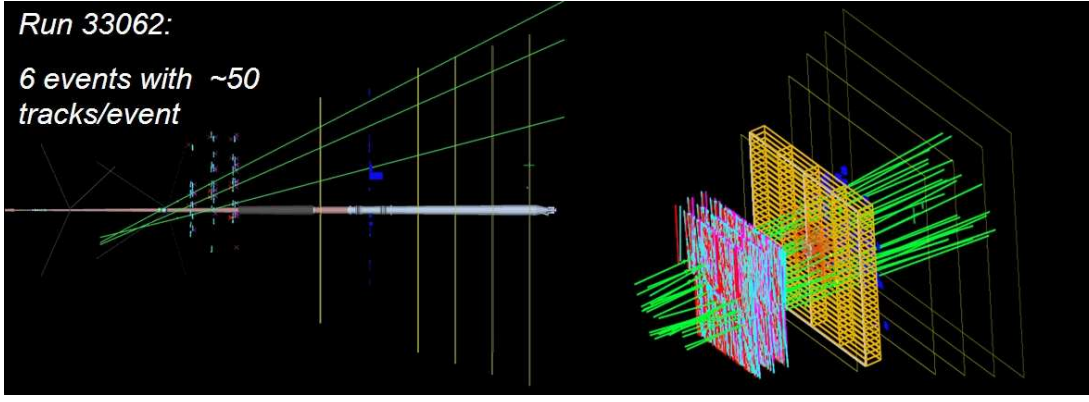


Figure 8: The beam-gas event collected from the first LHC beam circulation

15 minutes of data taking in the conditions expected for 2010. In total, in 2010 around 30M triggered, selected flavour tagged  $D^0 \rightarrow K^- \pi^+$  decays are expected. Also for 2010, around 2.5M of the triggered, selected flavour tagged  $D^0 \rightarrow K^+ K^-$  decays, essential for the  $y_{CP}$  parameter determination from lifetime measurements, should be collected. The expected event yield in 2010 exceeds significantly the number of about 110k  $D^0 \rightarrow K^+ K^-$  decays, collected by BELLE experiment with an integrated luminosity of  $540 \text{ fb}^{-1}$ . The  $D^0 \rightarrow h^+ h^-$  decays will be selected by two parallel analyses, one optimised for physics measurements, using the RICH, and the other with no particle identification criteria and with tighter kinematical requirements. The events from the latter selection will be invaluable for calibrating the RICH system. In addition, around 0.5M flavour tagged  $D^0 \rightarrow K^+ K^- \pi^+ \pi^-$  decays, up to a million flavour tagged  $D^0 \rightarrow K_S \pi^+ \pi^-$  decays and a few million  $D^+ \rightarrow K^+ K^- \pi^+$  events are expected in 2010.

One of the most sensitive ways to access the  $D\bar{D}$  mixing comes from the  $y_{CP}$  variable,

$$y_{CP} = \frac{\tau(D^0 \rightarrow K^- \pi^+)}{\tau(D^0 \rightarrow K^+ K^-)} - 1,$$

determination from the lifetime measurement for  $D^0 \rightarrow K^+ K^-$  and  $D^0 \rightarrow K^- \pi^+$  decays. The present HFAG average is  $y_{CP} = (1.107 \pm 0.217)\%$  [5]. However, so far no single  $5\sigma$  evidence of a non-zero value of the  $y_{CP}$  parameter exists, e.g. BELLE obtained [6]  $y_{CP} = (1.31 \pm 0.32 \pm 0.25)\%$  with an integrated luminosity of  $540 \text{ fb}^{-1}$ . Under the operation conditions expected for 2010, with the prompt  $D$  meson sample corresponding to  $0.1 \text{ fb}^{-1}$  integrated luminosity, the statistical error of the  $y_{CP}$  measurement at LHCb is expected to be 0.07%.

From the  $D^0 \rightarrow K^+ K^-$  sample also the  $CP$  violating parameter  $A_\Gamma$  can be measured,

$$A_\Gamma = \frac{\tau(\bar{D}^0 \rightarrow K^- K^+) - \tau(D^0 \rightarrow K^- K^+)}{\tau(\bar{D}^0 \rightarrow K^- K^+) + \tau(D^0 \rightarrow K^- K^+)}.$$

In the Standard Model  $A_\Gamma \leq 10^{-3}$ , while it can be as large as 1% with the New Physics contribution. The present

HFAG average is  $A_\Gamma(D^0 \rightarrow K^+ K^-) = (-1.6 \pm 2.3) \times 10^{-3}$  [5]. In 2010 with the prompt  $D$  meson sample corresponding to  $0.1 \text{ fb}^{-1}$  integrated luminosity, the expected LHCb statistical error is  $0.9 \times 10^{-3}$ .

The  $D\bar{D}$  mixing can also be studied measuring the wrong sign combinations,  $K^+ \pi^-$  corresponded to the initial  $D^0$ . The mixing followed by Cabibbo allowed decay,  $D^0 \rightarrow \bar{D}^0 \rightarrow K^+ \pi^-$ , is disentangled from doubly Cabibbo suppressed mode,  $D^0 \rightarrow K^+ \pi^-$ , using the time dependence,

$$\frac{dN_{ws}}{dt} \sim e^{-\Gamma t} \times \left( \frac{x'^2 + y'^2}{2} \cdot \frac{\Gamma^2 t^2}{2} + D_{DCS}^2 + D_{DCS} \cdot y' \cdot \Gamma t \right).$$

The study yields  $x'^2$  and  $y'$  mixing parameters. The proper time resolution curve for  $D^0 \rightarrow h^+ h^-$  from  $B$  decays can be fit with two Gaussians,  $\sigma_1 \sim 45 \text{ fs}$  and  $\sigma_2 \sim 111 \text{ fs}$  for 53% and 47% of entries correspondingly, Fig. 11. Fig. 12

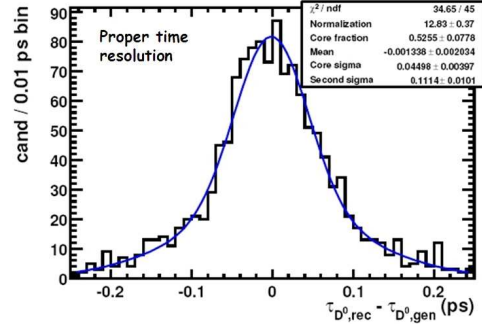


Figure 11: Proper time resolution curve for  $D^0 \rightarrow h^+ h^-$  from  $B$  decays

shows proper time distribution for the mixing, doubly Cabibbo suppressed decay, interference and background contributions from a toy Monte-Carlo study with the expected signal to background ratio of 0.4. In one nominal LHCb year the expected statistical error is  $1.4 \times 10^{-4}$  and  $1.9 \times 10^{-3}$  for  $x'^2$  and  $y'$  correspondingly. These statistical uncertainties are smaller than the statistical errors in the published results of B-factories with  $400 \text{ fb}^{-1}$  for

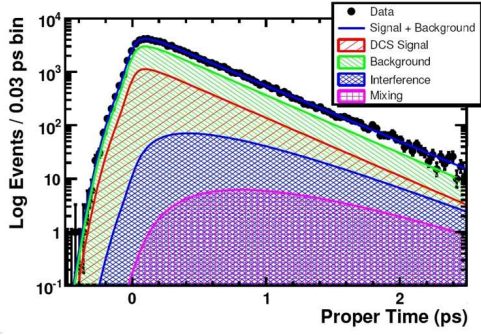


Figure 12: Proper time distribution for the wrong sign decays from a toy Monte-Carlo study with the expected signal to background ratio of 0.4. Contributions from mixing, doubly Cabibbo suppressed decay, interference and background are shown separately

BELLE [7] and  $384 \text{ fb}^{-1}$  for BaBar [8], and CDF [9] with  $1.5 \text{ fb}^{-1}$ .

Possible  $CP$  violation studies using the  $D^0 \rightarrow K^+ K^- \pi^+ \pi^-$  mode have been addressed in detail in [10]. The four-body final state gives access to additional observables, which can be accessed to search for  $CP$  violation in either a full amplitude analysis or a study of  $T$ -odd correlations. In one nominal LHCb year a sample of around 2M of the triggered and selected  $D^0 \rightarrow K^+ K^- \pi^+ \pi^-$  decays with  $D^0$  coming from  $B \rightarrow D^{*+}(\rightarrow D^0 \pi^+) X$  is expected. The  $D^0 \rightarrow K^+ K^- \mu^+ \mu^-$  is the most direct analogue of the kaon decay  $K_L \rightarrow \pi^+ \pi^- e^+ e^-$  in which  $T$ -odd asymmetry measurements were first pioneered. The measurement of  $BR(D^0 \rightarrow K^+ K^- \mu^+ \mu^-)$  can thus probe suppression mechanisms that can provide large  $T$ -odd asymmetry for the  $D^0 \rightarrow K^+ K^- \pi^+ \pi^-$  study. In one nominal LHCb year around 1k triggered and selected  $D^0 \rightarrow K^+ K^- \mu^+ \mu^-$  decays with  $D^0$  coming from  $B \rightarrow D^{*+}(\rightarrow D^0 \pi^+) X$  are expected for branching ratio of  $BR(D^0 \rightarrow K^+ K^- \mu^+ \mu^-) \sim 10^{-6}$ , for smaller values sensitivity can be limited by decays in flight from the  $D^0 \rightarrow K^+ K^- \pi^+ \pi^-$  mode. For both  $D^0 \rightarrow K^+ K^- \pi^+ \pi^-$  and  $D^0 \rightarrow K^+ K^- \mu^+ \mu^-$  modes, additional events from prompt  $D$  mesons can be exploited. In 2010 around 0.5M triggered, selected flavour tagged  $D^0 \rightarrow K^+ K^- \pi^+ \pi^-$  decays are expected, while a corresponding yield for  $D^0 \rightarrow K^+ K^- \mu^+ \mu^-$  is around a few hundred events.

Theoretical aspects of rare charm decays are addressed e.g. in [11]. The branching ratio of the decay,  $D^0 \rightarrow \mu^+ \mu^-$ , highly suppressed in the Standard Model ( $BR(D^0 \rightarrow \mu^+ \mu^-) < 10^{-12}$ ), can be significantly enhanced by many new physics models, in particular  $R$ -parity violating SUSY [12]. For  $BR(D^0 \rightarrow \mu^+ \mu^-) \sim 10^{-7}$ , below the BELLE limit [13] of  $BR(D^0 \rightarrow \mu^+ \mu^-) < 1.7 \times 10^{-7}$  @90%CL with an integrated luminosity of  $659 \text{ fb}^{-1}$ , LHCb already expects to have sensitivity down to the  $10^{-8}$  level with the 2010 dataset. Other rare  $D$  decays, e.g.  $D^+ \rightarrow X^+ l^+ l^-$ , are being studied.

The  $B_c^+$  mesons production rate at the LHC energy

of  $E_{CM} = 14 \text{ TeV}$  exceeds that at the Tevatron,  $\sigma(B_c)_{LHC}/\sigma(B_c)_{Tevatron} \sim O(10)$ . Thus about  $4 \times 10^8$   $B_c^\pm$  mesons will be produced per  $1 \text{ fb}^{-1}$  at LHCb, so that production cross section, mass and lifetime will be measured. The  $B_c^\pm$  mass measurement will use about 310  $B_c \rightarrow J/\psi(\rightarrow \mu^+ \mu^-)\pi$  decays with the resolution of about  $17 \text{ MeV}/c^2$ . Fig. 13 shows  $J/\psi \pi$  invariant mass dis-

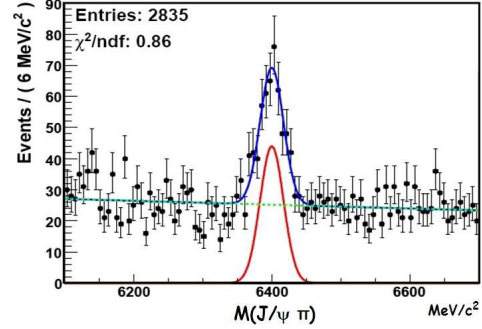


Figure 13:  $J/\psi \pi$  invariant mass distribution, with the expected  $B_c^+$  signal and background corresponding to  $1 \text{ fb}^{-1}$  sample

tribution, with the expected  $B_c^+$  signal and background corresponding to  $1 \text{ fb}^{-1}$  sample. The expected statistical error is  $1.7 \text{ MeV}/c^2$ . Thus the best-to-date result of CDF [14] based on  $2.4 \text{ fb}^{-1}$  sample can be improved. For the lifetime measurement about 360  $B_c \rightarrow J/\psi(\rightarrow \mu^+ \mu^-)\pi$  decays can be used. The proper time resolution is expected to be  $\sigma_\tau \sim 25 \text{ fs}$ . The  $1 \text{ fb}^{-1}$  sample will thus yield statistical error on the lifetime measurement of  $0.027 \text{ ps}$ . This is smaller than the best-to-date result of D0 [15] based on  $1.3 \text{ fb}^{-1}$  sample.

The study of production of charmonium states [16] at the LHCb takes advantage of the unique  $(p_T, \eta)$  coverage. Good separation between the prompt charmonium and the charmonium, coming from  $B$  decays, is achieved by using the  $t$  value:

$$t = \frac{dz}{p_z^{J/\psi}} \times m^{J/\psi},$$

which is very close to the  $b$  quark lifetime (Fig. 14). Fig. 15 shows the  $J/\psi$  signal over the background, dominated by the decays in flight, using the sample containing 19M minimum bias events after L0 trigger. The resolution of the  $J/\psi$  mass peak is  $\sigma = 11 \text{ MeV}/c^2$ , and signal to background ratio is about 4. Fig. 15 corresponds to  $1.1 \text{ s}$  LHCb operation at nominal luminosity. Early in the 2010 run even with a very small integrated luminosity, such as  $5 \text{ pb}^{-1}$ , several million of  $J/\psi$  containing events will be available for study. The sample will be used to measure the production cross section, both of the prompt  $J/\psi$ , and of  $b$  events through the secondary production, and to determine the  $J/\psi$  polarization, thus yielding an important tool to probe charmonium production mechanisms [17]. The systematic error from the luminosity measurement is expected

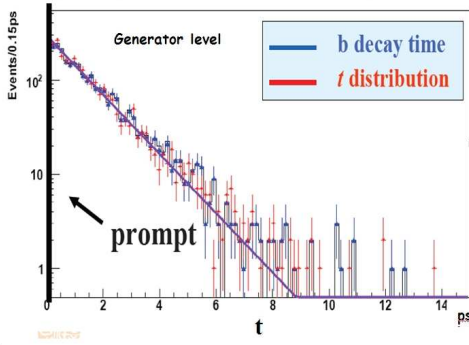


Figure 14: Separation between prompt  $J/\psi$  and  $J/\psi$  from  $b$  decays with the  $t$  variable

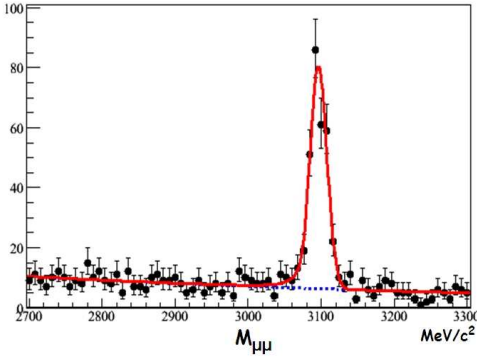


Figure 15:  $J/\psi$  signal after the L0 trigger from 19M minimum bias events over the expected background. It corresponds to the 1.1 s LHCb operation at nominal luminosity

to dominate the precision of the charmonium production studies.

Tevatron measurements show about 30% of  $J/\psi$  coming from the  $\chi_{c1,2}$  radiative decays. The relative production of  $J/\psi$  from  $\chi_{c1,2}$  and the relative  $\chi_{c1}$  to  $\chi_{c2}$  production will be studied in LHCb. Fig. 16 shows  $\Delta M = M(J/\psi \gamma) -$

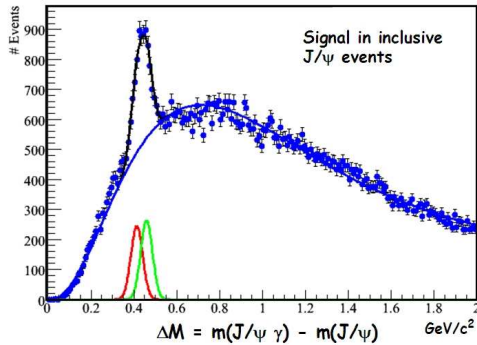


Figure 16: Mass difference  $\Delta M = M(J/\psi \gamma) - M(J/\psi)$ . Signal corresponds to the radiative  $\chi_{c1,2} \rightarrow J/\psi \gamma$  decay

$M(J/\psi)$  distribution for  $p_T > 0.5$  GeV/c, with a peak corresponding to the radiative  $\chi_{c1,2} \rightarrow J/\psi \gamma$  decay. The

mass resolution of  $\sigma \sim 27$  MeV/c<sup>2</sup> is smaller than the mass difference  $M(\chi_{c2}) - M(\chi_{c1}) = 55$  MeV/c<sup>2</sup>, so  $\chi_{c1}$  and  $\chi_{c2}$  separation should be feasible.

The power of the hadron machine to access new charmonium-like states was proven by CDF [18]. In addition, CDF concludes that about 84% of the  $X(3872)$  state comes from prompt production [19]. Triggering on dimuons from primary vertex with their invariant mass around  $M(J/\psi)$  and  $M(\psi(2S))$  will give access to the  $X(3872), Y(4010), Y(4260) \rightarrow J/\psi \pi\pi$  and  $Y(4350), Y(4660) \rightarrow \psi(2S) \pi\pi$  charmonium-like state decays correspondingly.

The access to the clean sample of  $X(3872)$  from  $B$  decays relies on the reconstruction of  $B^+ \rightarrow K^+ X(3872)$ , followed by  $X(3872) \rightarrow J/\psi \pi^+ \pi^-$ , with a branching fraction of about  $8 \times 10^{-6}$ . Note that the topology of this decay chain is similar to the core channel  $B^0 \rightarrow J/\psi K_S \rightarrow J/\psi \pi^+ \pi^-$ , and so trigger and reconstruction efficiencies are close. The expected event yield for  $X(3872)$  from  $B$  decays is thus about 10k events in one nominal year.

The charged  $Z^+(4430)$  state is accessed via  $\bar{B}^0 \rightarrow K^- Z^+(4430) \rightarrow K^- \psi(2S) \pi^+ \rightarrow K^- \mu^+ \mu^- \pi^+$  with a branching fraction of about  $3 \times 10^{-7}$ , and also topologically similar to  $B^0 \rightarrow J/\psi K_S \rightarrow \mu^+ \mu^- \pi^+ \pi^-$ . The expected event yield for  $Z^+(4430)$  from  $B$  decays is about 10k events in one nominal year.

## Conclusions

In summary, the LHCb experiment will enter the precision charm physics study club soon after the startup of LHC. Already with an integrated luminosity of  $5$  pb<sup>-1</sup>, the sample of about 3M  $J/\psi$  will be explored to attack measurements such as the prompt  $J/\psi$  cross section,  $J/\psi$  polarization,  $\chi_{c1,2}$  and  $\psi(2S)$  production, and  $X(3872)$  charmonium-like state. By the end of 2010, with about 100 pb<sup>-1</sup> integrated luminosity, a large number of signal events should be available for majority of the channels. Already with 100 pb<sup>-1</sup> LHCb has the possibility to make world best measurements of quantities such as  $y_{CP}$ . Finally, thereafter, LHCb will systematically deliver unprecedented precision to many studies of rare charm effects, with a nominal integrated luminosity of 2 fb<sup>-1</sup> per year.

## Acknowledgements

Present results are due to a joint work of many people from the LHCb collaboration, and it is my pleasure to acknowledge their important contribution. I am highly indebted to G. Wilkinson for useful discussions and to P. Buenitsky, V. Egorychev and G. Wilkinson for their invaluable help in preparing this paper.

## References

- [1] R. Antunes-Nobrega *et al.*, Reoptimized LHCb Detector, Design and Performance, CERN/LHCC/2003-030.

- [2] Throughout the paper charge conjugated states are also assumed.
- [3] R. Antunes-Nobrega *et al.*, LHCb Trigger System, CERN/LHCC/2003-031.
- [4] A. Augusto Alves *et al.*, JINST **3** (2008) S08005.
- [5] <http://www.slac.stanford.edu/xorg/hfag/charm/index.html>.
- [6] M. Staric *et al.*, Phys. Rev. Lett. **98** (2007) 211803.
- [7] L.M. Zhang *et al.*, Phys. Rev. Lett. **96** (2006) 151801.
- [8] B. Aubert *et al.*, Phys. Rev. Lett. **98** (2007) 211802.
- [9] T. Aaltonen *et al.*, Phys. Rev. Lett. **100** (2008) 121802.
- [10] I.I. Bigi, arXiv:0902.3048v1 (2009).
- [11] A. Petrov, *these proceedings*.
- [12] G. Burdman *et al.*, Phys. Rev. **D66** (2002) 014009.
- [13] E. Won, *talk at EPS HEP 2009*.
- [14] T. Aaltonen *et al.*, Phys. Rev. Lett. **100** (2008) 182002.
- [15] V.M. Abazov *et al.*, Phys. Rev. Lett. **102** (2009) 092001.
- [16] M. Nedden, *these proceedings*.
- [17] P. Artoisenet, *these proceedings*.
- [18] D.E. Acosta *et al.*, Phys. Rev. Lett. **93** (2004) 072001;  
T. Aaltonen *et al.*, Phys. Rev. Lett. **102** (2009) 242002.
- [19] G. Bauer, Int. J. Mod. Phys. **A20** (2005) 3765.